

UPPER EOCENE TO OLIGOCENE ISOTOPE
($^{87}\text{Sr}/^{86}\text{Sr}$, $\delta^{18}\text{O}$, $\delta^{13}\text{C}$) STANDARD SECTION,
DEEP SEA DRILLING PROJECT SITE 522

Kenneth G. Miller

Lamont-Doherty Geological Observatory
of Columbia University, Palisades, New York

Mark D. Feigenson

Department of Geological Sciences
Rutgers University, New Brunswick, New Jersey

Dennis V. Kent

Lamont-Doherty Geological Observatory
of Columbia University, Palisades, New York

Richard K. Olsson

Department of Geological Sciences
Rutgers University, New Brunswick, New Jersey

Abstract. We improved upper Eocene to Oligocene deep-sea chronostratigraphic control by integrating isotope ($^{87}\text{Sr}/^{86}\text{Sr}$, $\delta^{18}\text{O}$, $\delta^{13}\text{C}$) stratigraphy and magnetostratigraphy. Most previous attempts to establish the timing of isotope fluctuations have relied upon biostratigraphic age estimates which have uncertainties of 0.5 to over 4.0 m.y. Deep Sea Drilling Project (DSDP) Site 522 contains the best available upper Eocene to Oligocene magnetostratigraphic record which allows first-order correlations of isotope records ($^{87}\text{Sr}/^{86}\text{Sr}$, $\delta^{18}\text{O}$, $\delta^{13}\text{C}$) to the Geomagnetic Polarity Time Scale (GPTS). Empirical calibrations between the $^{87}\text{Sr}/^{86}\text{Sr}$ of foraminifera and magnetochronology at Site 522 allow more precise correlation of "unknown" samples with the GPTS. For example, shallow water and high-latitude sections may be tied into the deep-sea record. Sr-isotope stratigraphic resolution for the latest Eocene to Oligocene is approximately 2 m.y.

BACKGROUND

The advent of the Deep Sea Drilling Project and its successor the Ocean Drilling Program (ODP) provided recovery of relatively complete deep-sea sedimentary sequences. Since the pioneering work of Shackleton and Kennett [1975] and Savin et al. [1975], oxygen and carbon isotope measurements on these deep-sea sections have become routine for paleoceanographic and stratigraphic studies (see Miller et al., [1987] for a synthesis of Tertiary oxygen isotopes). Stratigraphic correlations using $\delta^{18}\text{O}$ and $\delta^{13}\text{C}$ records rely upon matching patterns of change, and therefore are usually not unique. More recently, studies by Burke et al. [1982], DePaolo and Ingram [1985], and Hess et al. [1986] have shown the potential for using the record of $^{87}\text{Sr}/^{86}\text{Sr}$ preserved

in marine carbonates as a stratigraphic tool. The Sr-isotope ratio in seawater is believed to be uniform at a given time, since the residence time is much longer than oceanic mixing times [Broecker and Peng, 1982]. A large increase in the $^{87}\text{Sr}/^{86}\text{Sr}$ record (~ 0.001300) measured in marine carbonates occurred from the late Eocene to Recent [Burke et al., 1982; DePaolo and Ingram, 1985; Hess et al., 1986]; hence, the Sr-isotope record has potential for chronostratigraphic correlations over the past 38 Ma.

Stratigraphic resolution is limited by the ability to tie records into a standard chronostratigraphic framework. A stratigraphic reference section provides a chronostratigraphic standard in which various records (including isotopes, biostratigraphy, and magnetostratigraphy) are directly correlated with one another, allowing these records to be tied into the geological time scale. In general, most isotope records have been correlated to the geological time scale using second- or third-order biostratigraphic correlations [e.g., DePaolo and Ingram, 1985]. Biostratigraphic correlations are often complicated by varying taxonomic and stratigraphic interpretations and by diachronous and geographically restricted ranges. Therefore, biostratigraphic age estimates require independent verification.

Magnetostratigraphy provides a facies-independent means of correlation which potentially yields virtually instantaneous temporal resolution near reversals. Advances in drilling technology have allowed recovery of several pre-Pliocene sections with good to excellent magnetostratigraphy [e.g., Tauxe et al., 1983]. Direct (first-order) correlations of biostratigraphy with magnetostratigraphy have led to an improved GPTS and an integrated geological time scale [Berggren et al., 1985]. Integration of isotope stratigraphy, biostratigraphy, and magnetostratigraphy into a chronostratigraphic standard [e.g., Miller et al., 1985a] is the first step toward developing the use of isotopes as a stratigraphic tool.

The late Eocene to Oligocene was an interval of important paleoceanographic and sea level changes [e.g., Miller et al.,

Copyright 1988 by the American Geophysical Union.

Paper number 8P0226.
0883-8305/88/008P-0226\$10.00

1985b], but stratigraphic control of Oligocene sections is often ambiguous because of long biozones in certain intervals. Sr-isotopes show a high rate of change [DePaolo and Ingram, 1985; Hess et al., 1986] and several global oxygen and carbon isotope fluctuations occurred during the late Eocene-Oligocene. Therefore, isotopes can provide improved correlations for this interval. DSDP Site 522 (eastern South Atlantic; 26° 7'S, 05° 8'W; 4441 m present water depth; ~3000-3800 m Oligocene water depth; ~2700 m late Eocene water depth) provides an excellent upper Eocene to Oligocene magnetostratigraphic record [Tauxe et al., 1983, 1984; Mead et al., 1986] with potential for developing a chronostratigraphic standard reference section [Hsu, LaBrecque et al., 1984]. We chose to focus on this section rather than other sections with good magnetostratigraphy (e.g., Contessa Quarry section; Lowrie et al. [1982]) because of its good carbonate preservation. Initial oxygen, carbon, and strontium isotope analyses of the upper Eocene to Oligocene have demonstrated the suitability of the Site 522 section [Poore and Matthews, 1984; Oberhänsli and Toumarkine, 1985; DePaolo and Ingram, 1985]. We have analyzed $^{87}\text{Sr}/^{86}\text{Sr}$, $\delta^{18}\text{O}$, and $\delta^{13}\text{C}$ composition of foraminiferal tests from this section, providing first-order calibrations of the isotope record with the GPTS.

METHODS

Magnetostratigraphy of Site 522 and its correlation to the GPTS is provided by Tauxe et al. [1983, 1984]. The time scale of Berggren et al. [1985] was used in making all age estimates. Samples for isotope analyses were soaked in hydrogen peroxide, washed with sodium hexametaphosphate in tap water through a 63- μm sieve, and air dried. Foraminifera were ultrasonically cleaned in deionized and distilled water (10-20 s for benthics, 3-10 s for planktonics). Oxygen and carbon isotope studies were performed on the benthic foraminifera *Cibicidoides* spp. (Figure 1; Table 1) which were picked from the greater than 150- μm -size fraction and roasted at 370°C in a vacuum. Studies have shown that this taxon accurately records $\delta^{13}\text{C}$ variations in seawater and is lower than $\delta^{18}\text{O}$ equilibrium by about 0.64 ‰ [e.g., Shackleton and Opdyke, 1973; Graham et al., 1981]. The CaCO_3 was analyzed at Lamont-Doherty Geological Observatory by either a Carousel-48 automatic carbonate preparation device (R. Fairbanks, unpublished data, 1988) attached to a Finnigan MAT 251 or by standard procedures [e.g., Fairbanks and Matthews, 1978] on a VG Micromass 903E.

Sr-isotope studies were performed upon greater than ~200 specimens of mixed planktonic foraminiferal taxa picked from the greater than 150- μm size fraction and dissolved in 3N HCl. Standard ion exchange techniques [e.g., Hart and Brooks, 1974] were used to separate strontium for analysis on a VG Sector mass spectrometer at Rutgers University. Internal precision (intran variability) on the Sector is approximately ± 0.000011 (2 sigma; mean for 22 analyses at Site 522); external precision (inter-run variability) is on the order of ± 0.000030 or better (see discussion). DePaolo and Ingram [1985] reported four analyses from Site 522 (Figure 1; Table 2) together with values for NBS 987 of 0.710310. At Rutgers, NBS 987 is routinely measured as 0.710250; therefore, we subtracted 0.000060 from the data of DePaolo and Ingram [1985] to facilitate comparisons with our data from Site 522 (Figure 1, Table 2). The agreement between the two studies is excellent (Figure 1).

RESULTS AND DISCUSSION

Diagenesis

Preservation of foraminifera is very good in the upper Eocene to Oligocene section at Site 522. There is no optical evidence of diagenesis, although several levels of intense dissolution occur in the section [Hsu, LaBrecque et al., 1984]. Our measurements of carbon and oxygen isotopes compare well with those of Poore and Matthews [1984] at Site 522 (Figure 1, Table 1). Our results are similar to those obtained from coeval sections with substantially different burial histories [e.g., Miller et al., 1987], suggesting little diagenetic overprinting of the upper Eocene to Oligocene section at Site 522. This is supported further by the good agreement of the Sr-isotope measurements within Site 522 (this study; cf. DePaolo and Ingram [1985]; Figure 1) and between different sites (Sites 522 and 516; see below).

Oxygen and Carbon Isotopes

Benthic foraminiferal (*Cibicidoides*) $\delta^{18}\text{O}$ values increase by about 0.6-1.0 ‰ in the lowermost Oligocene section at Site 522 (~133 m subbottom (msb)). High $\delta^{18}\text{O}$ values (>1.8 ‰) occur in the lowermost Oligocene (~126-133 msb) and subsequently decrease at ~125 msb. The lowermost Oligocene $\delta^{18}\text{O}$ increase occurs in normally magnetized sediments correlated with Chron C13n (Figure 1). Oberhänsli et al. [1984] observed a similar $\delta^{18}\text{O}$ increase in the benthic foraminiferal taxon *Stilostomella* spp. at this level at Site 522. The $\delta^{18}\text{O}$ increase has been widely reported from basal Oligocene sediments throughout the world [e.g., Kennett and Shackleton, 1976; Corliss et al., 1984; Miller et al., 1985c; Corliss and Keigwin, 1986; Keigwin and Corliss, 1986] and may be attributed to both a bottom water temperature drop and an increase in ice volume [Miller et al., 1987]. The only unambiguous first-order correlation of this $\delta^{18}\text{O}$ increase with the GPTS is at Site 522 [Oberhänsli et al., 1984; this study], yielding an age estimate of 35.7-35.9 Ma (Table 1).

Benthic foraminiferal $\delta^{13}\text{C}$ values also increase at the base of the Oligocene at 133 msb, with maximum values of ~1.5 ‰ in *Cibicidoides* occurring in sediments correlated with Chron C13n (35.8-35.3 Ma; Figure 1). Oberhänsli et al. [1984] observed high $\delta^{13}\text{C}$ values in *Stilostomella* spp. at this level at Site 522, although the relationship of this taxon with seawater $\delta^{13}\text{C}$ variations is not well known. Carbon isotope values subsequently begin to decrease at about 128 msb (earliest Chron C12r; circa 35 Ma), attaining a distinct minimum (Figure 1) which characterizes much of the Oligocene throughout the oceans. The global decrease in $\delta^{13}\text{C}$ values on a million-year scale cannot be attributed to transient reservoir changes such as occurred in the Quaternary [Broecker, 1982]. Rather, the change must be due to either a lowering of riverine $\delta^{13}\text{C}$ values or a decrease in the amount of organic carbon stored in sediments relative to carbonates [Miller and Fairbanks, 1985].

Previous studies of Pacific DSDP Sites 77 and 574 established that one or more intervals of high $\delta^{18}\text{O}$ values occurred in the "middle" Oligocene [Keigwin and Keller, 1984; Miller and Thomas, 1985]. Magnetostratigraphic and isotope studies at North Atlantic Site 558 suggested that high $\delta^{18}\text{O}$ values occurred in Chrons C11 and C9, although diagenetic problems limited use of this record [Miller and Fairbanks,

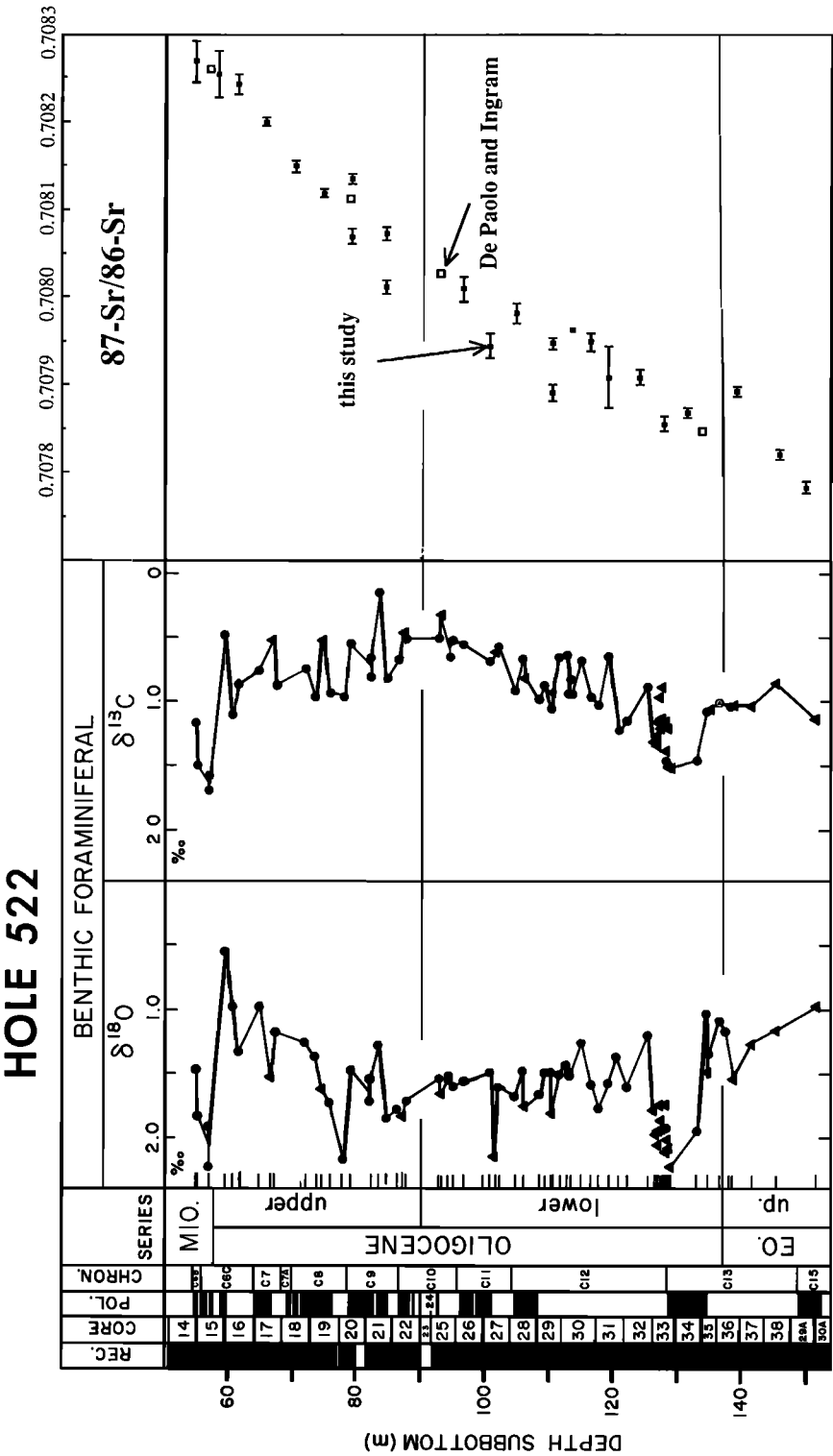


Fig. 1. Upper Eocene to lowermost Miocene isotope stratigraphy plotted versus subbottom depth and magnetostratigraphy at Site 522. Shaded intervals in REC indicate recovery. Magnetostratigraphy after Tauxe et al. [1983]; normal polarities are indicated by shading and reversed polarities are indicated by open intervals. Oxygen and carbon isotope data are indicated with circles (this study) and triangles [Poore and Mathews, 1984], and reported to the PDB standard. Sr-isotope data indicated with solid squares (this study) and open squares [DePaolo and Ingram, 1985]. Error bars reflect internal machine precision (intrarun variability) for each analysis (Table 2) and do not reflect interrun variability which is shown on Figure 2. Tick marks indicate levels of samples examined for stable isotopes. Chronostratigraphic boundaries are drawn on the basis of magnetostratigraphy and biostratigraphy [Poore, 1984], using the time scale of Berggren et al. [1985]. Cores are from Hole 522 with the exception of Cores 29A and 30A, which are from Hole 522A.

TABLE 1. Benthic Foraminiferal Oxygen and Carbon Isotope Data, Site 522

Sample	Depth, msb	Age, Ma	Lab	$\delta^{18}\text{O}_{\text{PDB}}^{\text{‰}}$	$\delta^{13}\text{C}_{\text{PDB}}^{\text{‰}}$
14-3, 122-125 cm	54.92	22.88	L-DGO	1.474	1.168
14-CC	55.10	22.98	L-DGO	1.832	1.491
15-2, 33-37	56.93	23.52	L-DGO	2.226	1.628
	56.93	23.52	L-DGO	1.91	1.69
15-CC	59.40	24.26	L-DGO	0.56	0.49
16-1, 110-114	60.60	24.58	L-DGO	0.98	1.10
16-2, 60-65	61.60	24.86	L-DGO	1.33	0.87
17-1, 84-88	64.74	25.67	L-DGO	0.98	0.76
17-2, 105-107	66.45	26.00	B	1.54	0.53
17-3, 25-29	67.15	26.14	L-DGO	1.16	0.86
18-3, 74-78	72.04	27.19	L-DGO	1.260	0.74
19-1, 93-97	73.63	27.43	L-DGO	1.37	0.97
19-2, 30-32	74.50	27.56	B	1.62	0.52
19-3, 24-28	75.94	27.77	L-DGO	1.73	0.93
20-1, 54-58	77.84	28.87	L-DGO	2.163	0.947
20-2, 34-38	79.14	28.29	L-DGO	1.48	0.55
21-1, 83-87	82.13	28.87	L-DGO	1.72	0.81
21-1, 88-90	82.18	28.87	L-DGO	1.543	0.642
21-2, 55-59	83.37	29.11	L-DGO	1.276	0.140
21-3, 27-31	84.57	29.34	L-DGO	1.842	0.811
22-1, 53-57	86.26	29.67	L-DGO	1.779	0.671
22-2, 50-51	87.70	29.91	B	1.83	0.46
22-2, 55-58	87.76	29.92	L-DGO	1.707	0.504
25-1, 126-130	92.86	30.75	L-DGO	1.538	0.501
25-2, 33-35	93.43	30.84	B	1.66	0.32
25-2, 126-128	94.36	30.99	L-DGO	1.554	0.646
	94.36	30.99	L-DGO	1.518	0.527
25-3, 50-54	95.10	31.11	L-DGO	1.609	0.517
26-1, 105-109	96.65	31.35	L-DGO	1.583	0.545
27-1, 95-99	100.79	31.95	L-DGO	1.490	0.679
27-2, 39-41	101.69	32.08	B	2.15	0.61
27-2, 94-98	102.23	32.16	L-DGO	1.595	0.557
28-1, 62-66	104.82	32.52	L-DGO	1.68	0.91
28-2, 33-37	106.03	32.66	L-DGO	1.48	0.66
28-2, 40-42	106.10	32.67	B	1.76	0.81
28-CC	108.30	32.92	L-DGO	1.646	0.978
29-1, 75-79	109.35	32.91	L-DGO	1.49	0.86
29-2, 34-38	110.44	33.18	L-DGO	1.49	1.05
29-2, 56-58	110.66	33.20	B	1.81	0.93
29-3, 14-18	111.74	33.33	L-DGO	1.51	0.65
29-CC	112.80	33.45	L-DGO	1.44	0.63
30-1, 53-57	113.53	33.54	L-DGO	1.50	0.94
	113.53	33.54	L-DGO	1.49	0.83
30-2, 56-60	115.06	33.71	L-DGO	1.26	0.68
30-3, 51-55	116.51	33.89	L-DGO	1.59	0.96
31-1, 46-50	117.86	34.05	L-DGO	1.77	1.02
31-2, 43-47	119.33	34.22	L-DGO	1.57	0.65
31-3, 53-57	120.93	34.41	L-DGO	1.386	1.384
32-1, 76-80	122.56	35.60	L-DGO	1.599	1.140
	122.56	35.60	L-DGO	1.568	1.141
32-3, 50-54	125.55	34.95	L-DGO	1.20	0.88
33-1, 34-36	126.54	35.06	B	1.78	1.32
33-1, 74-76	126.94	35.11	B	1.97	1.15
33-1, 84-86	127.04	35.12	B	2.05	1.26
33-1, 95-97	127.15	35.14	B	1.95	1.34
33-1, 115-117	127.35	35.16	B	1.75	0.97
33-1, 134-136	127.54	35.18	B	1.87	1.21
33-1, 145-147	127.65	35.19	B	1.74	0.89
33-2, 20-22	127.90	35.22	B	1.94	1.17
33-2, 27-29	127.97	35.23	B	1.92	1.13
33-2, 38-40	128.08	35.24	B	2.11	1.15
33-2, 42-44	128.12	35.25	L-DGO	1.91	1.46
33-2, 59-61	128.29	35.27	B	2.11	1.38
33-2, 86-88	128.56	35.30	B	2.01	1.20

TABLE 1. (continued)

Sample	Depth, msb	Age, Ma	Lab	$\delta^{18}\text{O}_{\text{PDB}}\text{‰}$	$\delta^{13}\text{C}_{\text{PDB}}\text{‰}$
33-2, 100-102	128.70	35.31	B	2.08	1.51
33-2, 147-149	129.17	35.36	B	2.23	1.52
34-3, 33-37	133.03	35.75	L-DGO	1.94	1.46
35-1, 107-113	134.77	35.92	L-DGO	1.03	1.07
35-1, 113-115	134.83	35.92	B	1.48	1.05
35-2, 73-79	135.93	36.03	L-DGO	1.364	1.107
36-1, 49-55	136.69	36.10	L-DGO	1.09	1.00
36-2, 40-46	138.10	36.23	L-DGO	1.18	1.04
36-2, 97-99	138.67	36.28	B	1.54	1.03
37-2, 50-52	141.70	36.57	B	1.27	1.03
38-2, 32-34	145.52	36.93	B	1.16	0.85
38-2, 32-34	151.99	37.53	B	1.00	1.16

Lab: L-DGO, Lamont-Doherty Geological Observatory; B, Brown University [Poore and Matthews, 1984]; msb, meters subbottom; Ma, age in millions of years estimated to two decimal places to reflect relative ages of closely spaced samples. Ages were obtained by linearly interpolating between the following magnetochron boundaries [Tauxe et al., 1983]: 54.38 msb, 22.57 Ma, top of Chron C6Bn; 55.61 msb, 23.27 Ma, top of Chron C6cn1; 57.10 msb, 23.55 Ma, top of Chron C6cn2; 58.61 msb, 24.04 Ma, top of Chron C6cn3; 63.95 msb, 25.50 Ma, top of Chron C7; 68.34 msb, 26.38 Ma, top of Chron C7A; 69.86 msb, 26.86 Ma, top of Chron C8; 78.44 msb, 28.15 Ma, top of Chron C9; 86.59 msb, 29.73 Ma, top of Chron C10; 95.81 msb, 31.23 Ma, top of Chron C11; 104.35 msb, 32.46 Ma, top of Chron C12; 128.47 msb, 35.29 Ma, top of Chron C13; 134.25 msb, 35.87 Ma, Chron C13n2/C13r2; 148.88 msb, 37.24 Ma, top of Chron C15.

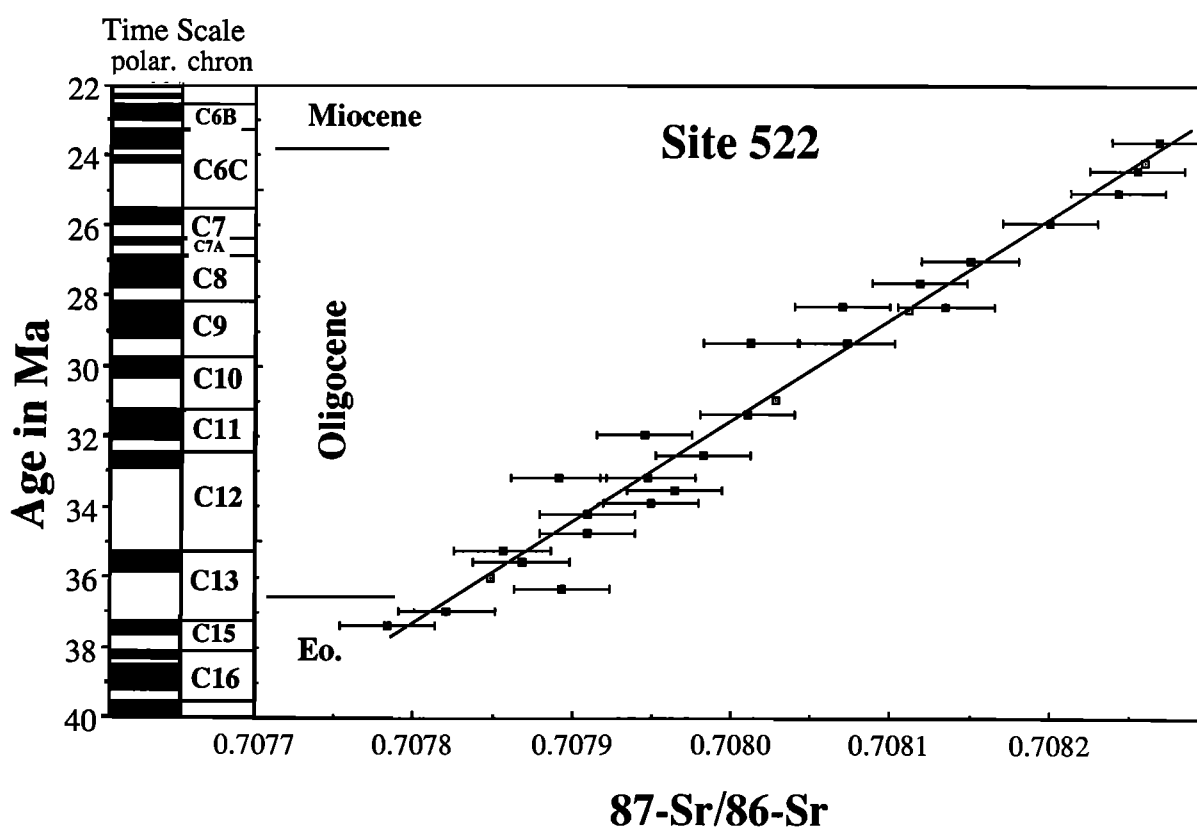


Fig. 2. Sr-isotope data versus age for Site 522. Data from Site 522 are indicated with solid squares [this study] and open squares [DePaolo and Ingram, 1985](Table 2). Linear regression was drawn on the basis of data from this study and data adjusted from DePaolo and Ingram [1985]. Error bars reflect our estimate of interrun variability, and a uniform error of ± 0.000030 was assigned to each point analyzed here (see text).

TABLE 2. Sr-isotope data

Sample	Depth, msb	Age, Ma	$^{87}\text{Sr}/^{86}\text{Sr}$
<i>This study</i>			
Site 522			
14-3, 122-125	54.92	23.69	0.708269±23
15-3, 30-34	58.40	24.39	0.708255±26
16-2, 61-65	61.61	25.03	0.708243±11
17-2, 54-58	65.94	25.90	0.708200±5
18-2, 73-77	70.53	26.96	0.708150±7
19-2, 62-66	74.82	27.61	0.708119±5
20-2, 34-38	79.14	28.29	0.708070±8
20-2, 34-38			0.708135±6
21-3, 27-31	84.57	29.34	0.708012±7
21-3, 27-31			0.708073±8
26-1, 105-109	96.65	31.35	0.708010±14
27-1, 95-99	100.75	31.94	0.707945±14
28-1, 62-66	104.82	32.52	0.707982±12
29-2, 34-38	110.44	33.17	0.707891±9
29-2, 34-38			0.707947±6
30-1, 53-57	113.53	33.54	0.707964±7
30-3, 51-55	116.51	33.89	0.707949±11
31-2, 43-47	119.33	34.22	0.707909±35
32-2, 75-79	124.05	34.77	0.707909±8
33-2, 42-44	128.12	35.25	0.707856±9
34-2, 30-34	131.50	35.59	0.707868±6
36-3, 12-18	139.32	36.34	0.707983±6
38-2, 92-97	146.12	36.98	0.707821±6
29A-2, 109-112	150.09	37.36	0.707784±7
Hole 548A*			
16-1, 39-41	348.39	28.7	0.708101±14
16-3, 66-69	351.66	32.7**	0.707961±11
16-4, 39-41	352.89	33.4	0.707934±9
Hole 549A*			
10-3, 40-43	87.40	30.9	0.708022±18
10-6, 143-148	92.93	34.4	0.707902±6
11-6, 143-148	102.43	34.6	0.707895±14
DePaolo and Ingram [1985]***			
Site 522			
15-2, 63	57.23	24.15	0.708260
20-2, 73	79.53	28.36	0.708112
25-2, 93	94.03	30.94	0.708028
35-2, 42	135.62	36.00	0.707848

*Ages for Sites 548 and 549 were estimated from the linear regression (Figure 2). **Although sample 16-3, 66-69 cm is located immediately above the disconformity at 16-3, 70 cm, its age estimate is closer to the sample below the disconformity due to the presence of abundant reworked lower Oligocene foraminifera. ***0.000060 was subtracted from values reported by DePaolo and Ingram [1985](see text); Ma, age in millions of years estimated to two decimal places for Site 522 to reflect relative ages of closely spaced oxygen and carbon isotope samples.

1985]. The "middle" Oligocene interval(s) of high $\delta^{18}\text{O}$ values is not well represented at Site 522 (Figure 1). High $\delta^{18}\text{O}$ values (> 2.0 ‰) occur at about 102 msb (Chron C11r; circa 32 Ma) and about 78 msb (Chron C8r; circa 29 Ma), but these are limited to single point peaks (Figure 1). The poor representation of the $\delta^{18}\text{O}$ increase at Site 522 may be partially due to the intense dissolution during Chron C11 at this location [Hsu, LaBrecque et al., 1984].

Both $\delta^{18}\text{O}$ and $\delta^{13}\text{C}$ values increase sharply near the top of the Oligocene in Chron C6Cn at Site 522 (Figure 1; between C6Cn1 and C6Cn3), followed by a sharp decrease. This distinctive geochemical signature has been noted previously at North Atlantic Sites 558 and 563 in latest Chron C6Cr [Miller

and Fairbanks, 1985]. Considering uncertainties in the magnetostratigraphy at Sites 558 and 563 [Miller et al., 1985a], we suggest that the $\delta^{18}\text{O}$ and $\delta^{13}\text{C}$ increases were synchronous at all three locations. We estimate that the increases occurred during Chron C6Cn1–C6Cn3 (23.5–24.3 Ma), an interval encompassing the Oligocene/Miocene boundary (23.7 Ma). We have subsequently identified this interval of high $\delta^{18}\text{O}$ and $\delta^{13}\text{C}$ values at equatorial Atlantic Sites 366 and 667 and South Atlantic Site 529; at all six Atlantic locations in which we have observed this change, $\delta^{18}\text{O}$ and $\delta^{13}\text{C}$ values increase immediately below the level of the first appearance of *Globorotalia kugleri* s.s., which is used to recognize the Oligocene/Miocene boundary [Berggren et al.,

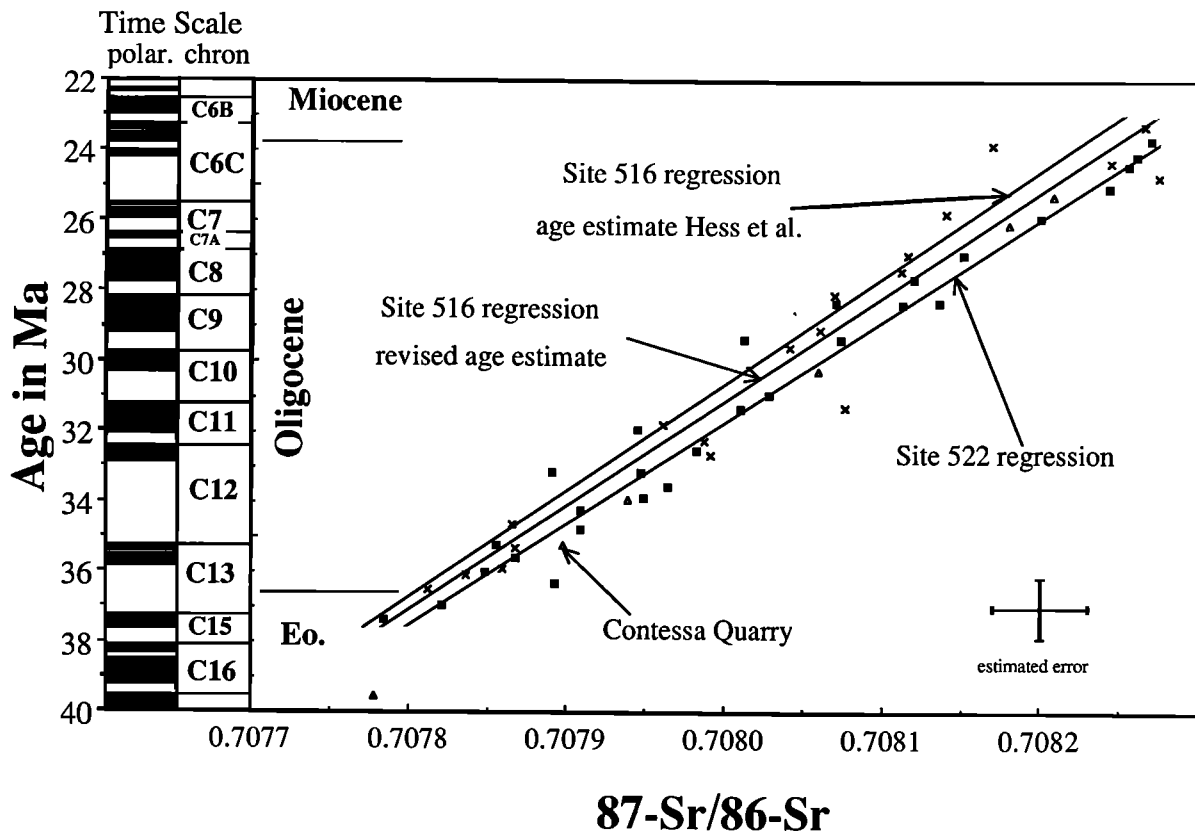


Fig. 3. Data and regression from Site 522 (solid squares) are compared with data from Site 516 (x's; Hess et al. [1986]) and Contessa Quarry [DePaolo and Ingram, 1985] for the interval 40–22 Ma. Error bars are applicable to our data and represent our estimate of interrun variability (± 0.000030) and the corresponding age uncertainty (± 0.85 m.y.), given the rate of change of $0.000035/\text{m.y.}$ (see text). Regression lines were individually computed for Sites 522 (as in Figure 2) and 516. Two regression lines were computed for Site 516: (1) using the age estimates of Hess et al. [1986] (data not shown); and (2) using revised age estimates (data plotted as x's) obtained by linearly interpolating between the following levels. First Occurrence (FO) *Orbulina* spp., 73 msb, 15.2 Ma; FO *G. sicanius*, 95 msb, 16.6 Ma; Last Occurrence (LO) *C. dissimilis*, 107 msb, 17.6 Ma; LO *G. kugleri*, 173 msb, 21.8 Ma; LO *Gt. opima opima*, 309 msb, 28.2 Ma; LO *Chiloguembulina* spp., 354 msb, 30.0 Ma; LO *Pseudohastigerina* spp., 458 msb, 34.0 Ma; LO *Gt. cerroazulensis cerroazulensis*, 538 msb, 36.6 Ma; LO *Gt. spinulosa*, 633 msb, 41.1 Ma; top Chron C20, 786 msb, 44.66 Ma; top Chron C21, 833 msb, 48.75 Ma. Biostratigraphic levels after Pujol [1983] and Berggren et al. [1983a, b].

1985]. Thus, the $\delta^{18}\text{O}$ and $\delta^{13}\text{C}$ increases allow relatively precise recognition of the Oligocene/Miocene boundary interval in pelagic sections.

Sr-Isotopes

The ratio of $^{87}\text{Sr}/^{86}\text{Sr}$ has generally increased since the late Eocene [Burke et al., 1982; DePaolo and Ingram, 1985; Hess et al., 1986]. It is not clear whether this increase has been strictly monotonic or if there were higher-order variations (million-year scale or shorter) [DePaolo, 1986; Hodell and Muller, 1988]. Our studies of the upper Eocene to Oligocene section at Site 522 show increasing $^{87}\text{Sr}/^{86}\text{Sr}$ values (Figure 1) with an overall change of approximately 0.000500 over this 14.5 m.y. of record (Figure 1).

It is necessary to determine a relationship between $^{87}\text{Sr}/^{86}\text{Sr}$

and age in order to use Sr-isotopes for chronostratigraphic correlations. The cause(s) of changing $^{87}\text{Sr}/^{86}\text{Sr}$ through time are not well known (mechanisms include changing continental weathering, hydrothermal flux, and carbonate recycling; see Elderfield [1986] for review). Hence, relationships between Sr-isotope variations and age must be empirically determined. We did this by estimating the ages of our $^{87}\text{Sr}/^{86}\text{Sr}$ measurements at Site 522 using magnetostratigraphy (linearly interpolating between depth-age pairs for Chron boundaries; Table 1). A linear relationship provides an excellent fit to the late Eocene to Oligocene Sr-isotope record (Figure 2), with a mean rate of change of $0.000035/\text{m.y.}$ Use of higher-order functions does not significantly improve the fit. We used a linear relationship to estimate the ages of strata by measuring their $^{87}\text{Sr}/^{86}\text{Sr}$ composition:

$$\text{Age (Ma)} = 20392.79 - 28758.84 (^{87}\text{Sr}/^{86}\text{Sr}) \quad (1)$$

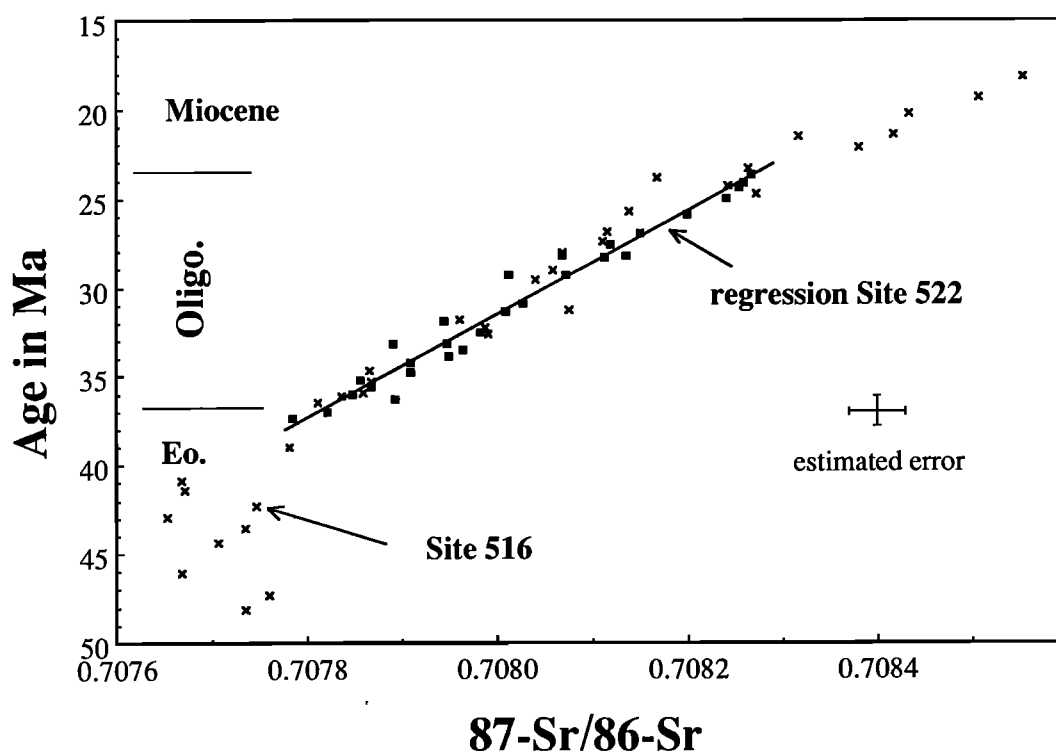


Fig. 4. Data and regression from Site 522 (solid squares) are compared with data from Site 516 (x's; Hess et al. [1986]) for the interval 50-15 Ma using revised age estimates for Site 516 (Figure 2). Regression line for Site 522 as in Figure 2. Note different scales between Figures 3 and 4. Estimated errors as in Figure 3.

Our measurements do not address the nature of the Sr-isotope record on time scales shorter than about 2 m.y., and higher-order variability such as that observed in the Neogene [DePaolo, 1986; Hodell and Muller, 1988] may be hidden by our sampling interval.

We compared the Site 522 $^{87}\text{Sr}/^{86}\text{Sr}$ record with the best previously published Eocene to Oligocene time series, western South Atlantic Site 516 [Hess et al., 1986]. Using the age estimates of Hess et al. [1986] yields good agreement between the $^{87}\text{Sr}/^{86}\text{Sr}$ records at Sites 516 and 522, and the regression lines for the individual sites computed for the interval 38-22 Ma are similar (Figure 3). As part of ongoing studies of Oligocene magnetobiostratigraphy, we refined age estimates for Site 516, relying more heavily upon biostratigraphy [Pujol, 1983; Berggren et al., 1983a, b] because the magnetostratigraphy for this site is equivocal at certain levels [Berggren et al., 1983a, b; D. V. Kent and K. G. Miller, unpublished data, 1988]. Our age estimates for Site 516 differ from those of Hess et al. [1986] primarily in the interval 30-25 Ma during which the maximum difference between age estimates is less than 1 m.y. (age model in Figure 3 caption). Comparison between the records at Site 522 and the revised age estimates at Site 516 shows excellent agreement (Figure 3). The data from Site 516 generally fall within ± 0.000030 of the Site 522 regression; only three points fall outside of ± 0.000050 of the Site 522 regression (Figure 3).

The Site 522 data and regression also compare well with Sr-isotope data from Contessa Quarry [DePaolo and Ingram, 1985]. The five data points from Contessa Quarry which lie

between 38 and 22 Ma fall within ± 0.000030 of the Site 522 regression (Figure 3). The excellent agreement among $^{87}\text{Sr}/^{86}\text{Sr}$ records occurs among three sections with different burial histories (Figure 3): the upper Eocene-Oligocene section at Site 522 consists of a shallowly buried (~50-150 m) soft sticky ooze [Hsu, Labrecque et al., 1984]; the coeval section at Site 516 (~200-600 m) ranges from an ooze to a well lithified chalk to a limestone [Barker et al., 1983]; and the coeval Scaglia Variegata-Scaglia Cinerea section at Contessa Quarry ranges from an indurated marl to a limestone [Lowrie et al., 1982]. The Sr-isotope similarity among records from such diversely lithified units argues that diagenetic problems are not severe in these sections (see also DePaolo and Ingram's [1985] figure 1).

Evaluating temporal resolution of Sr-isotope stratigraphy is dependent upon the rate of change of $^{87}\text{Sr}/^{86}\text{Sr}$ through time and the ability to measure $^{87}\text{Sr}/^{86}\text{Sr}$ in carbonates. External machine precision for the VG Sector is judged to be ± 0.000030 or better for two reasons: (1) 12 of our measurements of the NBS 987 standard have a 2 sigma deviation of 0.000024; and (2) our measurements at Site 522 fall within ± 0.000030 of the regression line with the exception of five data points. These five data points may represent large, short-period seawater fluctuations; however, replicates of three of these samples (Table 2) fall within ± 0.000030 of the regression. We have used ± 0.000030 as an estimate for our error on Figures 1-4, which is a conservative estimate that exceeds the within-run variability (Table 2). Given the mean rate of change of $^{87}\text{Sr}/^{86}\text{Sr}$ for the late Eocene

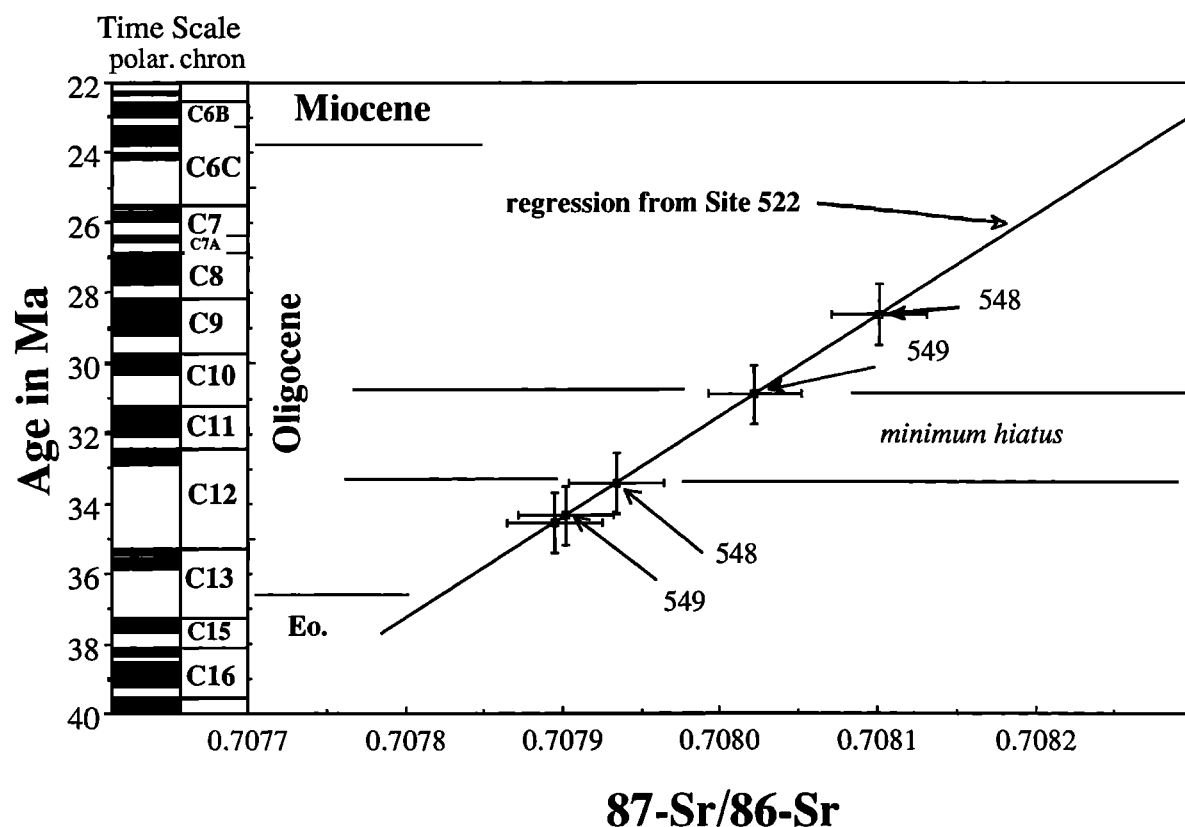


Fig. 5. An example using Sr-isotope stratigraphy to determine ages of samples from Irish margin Sites 548 (open squares) and 549 (solid squares). Samples from Sites 548 and 549 were measured for $^{87}\text{Sr}/^{86}\text{Sr}$ and plotted on the regression line from Site 522 based upon their Sr-isotope composition. Estimated ages for the samples from Sites 548 and 549 are determined from the regression line. Based upon this, we delineate hiatuses at both sites (Site 548 from circa 33-28 Ma; Site 549 from circa 34-30.5 Ma). Minimum hiatus of 33-30.5 Ma was determined by combining age estimates of hiatuses at both sites. Estimated errors as in Figure 3.

to Oligocene of 0.000035/m.y., this corresponds to a 1.7-m.y. resolution (Figure 5). This is similar to or better than biostratigraphic resolution, which varies from approximately 0.5 to 4 m.y. in the Oligocene [Berggren et al., 1985].

The age versus Sr-isotope regression established at Site 522 appears valid only from 38 Ma (latest Eocene) to 22 Ma (earliest Miocene) (Figure 4). The Site 516 data show that the rate of change of $^{87}\text{Sr}/^{86}\text{Sr}$ increased during the early Miocene and that the late Eocene-Oligocene regression is not applicable to the early Miocene (Figure 4). The higher rate of change of $^{87}\text{Sr}/^{86}\text{Sr}$ during the early Miocene potentially affords greater stratigraphic resolution than possible for the Oligocene. Also, as noted by Hess et al. [1986], there is high variability but no apparent trend in the $^{87}\text{Sr}/^{86}\text{Sr}$ ratio during the middle to early late Eocene (between 50 and 38 Ma the ratio was 0.707700 ± 0.000070). Sr-isotopes may not be useful for Eocene stratigraphy, although the Sr-isotope record of this interval is poorly known.

We provide one example of the use of Sr-isotope stratigraphy for improving geological correlations. We have reported on a hiatus that occurred in the "middle" Oligocene at DSDP Sites 548 and 549 on the Irish continental margin (Goban Spur) [Miller et al., 1985b, c]. Using biostratigraphy, we estimated that the minimum hiatus at these sites was from

34 to 30 Ma. Measurements of $^{87}\text{Sr}/^{86}\text{Sr}$ at Site 548 were conducted above and below a distinct lithologic disconformity associated with the hiatus [Poag et al., 1985]. The ages for the $^{87}\text{Sr}/^{86}\text{Sr}$ values can be estimated from the linear regression (Figure 2) as approximately 28.6 Ma above the disconformity and 33.4 Ma below the disconformity, within 1 m.y. of the biostratigraphic age estimates (i.e., Zones NP24 and P21B above, 30.0-28.2 Ma; Zones NP22 and P18 below, 35.1-34.0 Ma; Miller et al. [1985b, c]). No physical disconformity was noted at Site 549, but biostratigraphic studies suggest a hiatus [Miller et al., 1985c]. Sr-isotope stratigraphic estimates place the hiatus at this site between 34.4 and 30.8 Ma (Figure 5; between samples 10-6, 134 cm and 10-3, 40 cm). We originally believed that the break occurred between sample 10-6, 143 cm and 11-6, 143 cm [Miller et al., 1985c], but the Sr-isotope stratigraphy suggests that the break occurred within core 10. This is consistent with biostratigraphy, which suggests that sample 11-6, 143 cm represents Zones NP22 and P18 (35.1-34.8 Ma), sample 10-6, 143 cm is problematical, and sample 10-3, 40 cm is near the boundary of Zones P19/20 and P21A (~31.5-30.5 Ma). The agreement between the Sr-isotope stratigraphic and biostratigraphic estimates as to the ages of the hiatuses is excellent (Figure 5), especially considering the resolution afforded by each method.

With the potential for discriminating approximately 2-m.y. intervals for the late Eocene to Oligocene, Sr-isotope stratigraphy alone is a powerful stratigraphic tool. However, the real power of Sr-isotope stratigraphy lies in integration with all available stratigraphic techniques. Integration of Sr-isotope stratigraphy with magnetostratigraphy, biostratigraphy, and oxygen and carbon isotope stratigraphy promises to yield late Eocene-Oligocene resolution better than 1 m.y. The greatest potential for such integrated stratigraphy lies in applications to difficult geological settings/problems: (1) linking pelagic sections with shallow-marine and high-latitude sections; (2) providing means for deciphering diachrony of taxa; and (3) sorting out problems due to coring and/or to shallow water facies.

SUMMARY

Upper Eocene to Oligocene isotope records ($^{87}\text{Sr}/^{86}\text{Sr}$, $\delta^{18}\text{O}$, $\delta^{13}\text{C}$) at Site 522 can be directly correlated to the Geomagnetic Polarity Time Scale. Among the most diagnostic stratigraphic changes are two sharp increases in both $\delta^{18}\text{O}$ and $\delta^{13}\text{C}$ which occur near the base (earliest Chron C13n; 35.8 ± 0.1 Ma) and the top (Chron C6Cr1-C6Cn3; 23.9 ± 0.4 Ma) of the Oligocene; these are global changes which provide stratigraphic correlations among deep-sea sections. "Middle" Oligocene intervals of high $\delta^{18}\text{O}$ values noted elsewhere are not fully resolved at this site due to dissolution, but high $\delta^{18}\text{O}$ values apparently occurred in Chron C11r (circa 32 Ma) and C8r-C9n (circa 29 Ma).

First-order calibrations of the $^{87}\text{Sr}/^{86}\text{Sr}$ record with the GPTS at Site 522 establish an Oligocene chronostratigraphic tool with a resolution (approximately 2 m.y.) comparable to or better than biostratigraphy. We used the Sr-isotope stratigraphic technique to estimate the age of a hiatus noted in two boreholes on the Irish margin and found that these estimated ages confirmed biostratigraphic estimates. Sr-isotope stratigraphy should prove to be quite useful in improving correlations of shallow water and high-latitude sections to the GPTS.

Acknowledgments. We thank S. M. Savin and D. A. Hodell for reviews, R. G. Fairbanks for providing the oxygen and carbon isotope data, M.-P. Aubry, W. A. Berggren, and J. Hess for discussions, and M. E. Katz, C. Skuba, and A. N. Brower for technical assistance. This work was supported by National Science Foundation grants OCE85-00859 and OCE87-00005 (Miller and Kent) and OCE86-14508 (Kent). This is Lamont-Doherty Geological Observatory contribution 4288.

REFERENCES

- Barker, P. R., R. L. Carlson, and D. A. Johnson, et al., *Initial Rep. Deep Sea Drill. Proj.*, 72, 1024 pp., 1983.
- Berggren, W. A., M. P. Aubry, and N. Hamilton, Neogene magnetobiostratigraphy of Deep Sea Drilling Project Site 516 (Rio Grande Rise, South Atlantic), Deep Sea Drilling Project Leg 72, *Initial Rep. Deep Sea Drill. Proj.*, 72, 675-713, 1983a.
- Berggren, W. A., N. Hamilton, D. A. Johnson, C. Pujol, W. Weiss, P. Cepek, and A. M. Gombos, Jr., Magnetobiostratigraphy of Deep Sea Drilling Project Leg 72, Sites 515-518, Rio Grande Rise (South Atlantic), *Initial Rep. Deep Sea Drill. Proj.*, 72, 939-948, 1983b.
- Berggren, W. A., D. V. Kent, and J. J. Flynn, Paleogene geochronology and chronostratigraphy, *Mem. Geol. Soc. London*, 10, 141-195, 1985.
- Broecker, W. S., Ocean chemistry during glacial time, *Geochim. Cosmochim. Acta*, 46, 1689-1705, 1982.
- Broecker, W. S., and T.-H. Peng, *Tracers in the Sea*, 690 pp., Eldigio Press, Palisades, New York, 1982.
- Burke, W. H., R. E. Denison, E. A. Hetherington, R. B. Koepnick, H. F. Nelson, and J. B. Otto, Variation of seawater $^{87}\text{Sr}/^{86}\text{Sr}$ throughout Phanerozoic time, *Geology*, 10, 516-519, 1982.
- Corliss, B. H., and L. D. Keigwin, Eocene-Oligocene paleoceanography, in *Mesozoic and Cenozoic Oceans*, *Geodyn. Ser.*, vol. 15, edited by K. J. Hsu, pp. 101-118, AGU, Washington, D. C., 1986.
- Corliss, B. H., M. P. Aubry, W. A. Berggren, J. M. Fenner, L. D. Keigwin, and G. Keller, The Eocene/Oligocene boundary event in the deep sea, *Science*, 226, 806-810, 1984.
- DePaolo, D. J., Detailed record of the Neogene Sr isotopic evolution of seawater from DSDP Site 590B, *Geology*, 14, 103-106, 1986.
- DePaolo, D. J., and B. L. Ingram, High-resolution stratigraphy with strontium isotopes, *Science*, 227, 938-940, 1985.
- Elderfield, H., Strontium isotope stratigraphy, *Palaeogeogr. Palaeoclimatol. Palaeoecol.*, 57, 71-90, 1986.
- Fairbanks, R. G., and R. K. Matthews, The marine oxygen isotopic record in Pleistocene coral, Barbados, West Indies, *Quat. Res.*, 10, 181-196, 1978.
- Graham, D. W., B. H. Corliss, M. L. Bender, and L. D. Keigwin, Carbon and oxygen isotopic disequilibria of Recent benthic foraminifera, *Mar. Micropaleontol.*, 6, 483-497, 1981.
- Hart, S. R., and C. Brooks, Clinopyroxene-matrix partitioning of K, Rb, Cs, and Ba, *Geochim. Cosmochim. Acta*, 38, 1799-1806, 1974.
- Hess, J., M. L. Bender, and J.-G. Schilling, Evolution of the ratio of strontium-87 to strontium-86 in seawater from Cretaceous to Present, *Science*, 231, 979-984, 1986.
- Hsu, K., J. LaBrecque, et al., *Initial Rep. Deep Sea Drill. Proj.*, 73, 798, 1984.
- Hodell, D. A., and P. A. Muller, Strontium isotope stratigraphy and geochemistry of the Late Neogene ocean (9 to 2 Ma), *Earth Planet. Sci. Lett.*, in press, 1988.
- Keigwin, L. D., and B. H. Corliss, Stable isotopes in Eocene/Oligocene foraminifera, *Geol. Soc. Am. Bull.*, 97, 335-345, 1986.
- Keigwin, L. D., and G. Keller, Middle Oligocene climatic change from equatorial Pacific DSDP Site 77, *Geology*, 12, 16-19, 1984.
- Kennett, J. P., and N. J. Shackleton, Oxygen isotope evidence for the development of the psychrosphere 38 Myr ago, *Nature*, 260, 513-515, 1976.
- Lowrie, W., W. Alvarez, G. Napoleone, K. Perch-Nielsen, I. Premoli-Silva, and M. Toumarkine, Paleogene magnetic stratigraphy in Umbrian pelagic carbonate rocks: The Contessa sections, Gubbio, *Geol. Soc. Am. Bull.*, 93, 414-432, 1982.
- Mead, G. A., L. Tauxe, and J. LaBrecque, Oligocene paleoceanography of the south Atlantic: Paleoclimatic implications of sediment accumulation rates and magnetic susceptibility measurements, *Paleoceanography*, 1, 273-284, 1986.
- Miller, K. G., and R. G. Fairbanks, Oligocene-Miocene global carbon and abyssal circulation changes, in *The Carbon*

- Cycle and Atmospheric CO₂: Natural Variations Archean to Present*, *Geophys. Monogr. Ser.*, vol. 32, edited by Sundquist, E., and W. S. Broecker, pp. 469-486, AGU, Washington, D. C., 1985.
- Miller, K. G., and E. Thomas, Late Eocene to Oligocene benthic foraminiferal isotopic record, Site 574 equatorial Pacific, *Initial Rep. Deep Sea Drill. Proj.*, 85, 771-777, 1985.
- Miller, K. G., M. P. Aubry, M. J. Khan, A. J. Melillo, D. V. Kent, and W. A. Berggren, Oligocene to Miocene biostratigraphy, magnetostratigraphy, and isotopic stratigraphy of the western North Atlantic, *Geology*, 13, 257-261, 1985a.
- Miller, K. G., G. S. Mountain, and B. E. Tucholke, Oligocene glaciocustasy and erosion on the margins of the North Atlantic, *Geology*, 13, 10-13, 1985b.
- Miller, K. G., W. B. Curry, and D. R. Ostermann, Late Paleogene benthic foraminiferal paleoceanography of the Goban Spur Region, DSDP Leg 80, *Initial Rep. Deep Sea Drill. Proj.*, 80, 505-538, 1985c.
- Miller, K. G., R. G. Fairbanks, and G. S. Mountain, Tertiary oxygen isotope synthesis, sea level history, and continental margin erosion, *Paleoceanography*, 1, 1-19, 1987.
- Oberhänsli, H., and M. Toumarkine, The Paleogene oxygen and carbon isotope history of Sites 522, 523, and 524 from the central South Atlantic, eds., in *South Atlantic Paleoceanography*, edited by K. J. Hsu and H. J. Weissert, pp. 125-147, Cambridge University Press, New York, 1985.
- Oberhänsli, H., J. McKenzie, M. Toumarkine, and H. Weissert, A paleoclimatic and paleoceanographic record of the Paleogene in the central South Atlantic (Leg 73, Sites 522, 523, and 524), *Initial Rep. Deep Sea Drill. Proj.*, 73, 737-747, 1984.
- Poag, C. W., L. A. Reynolds, J. M. Mazzullo, and L. D. Keigwin, Foraminiferal, lithic, and isotopic changes across four major unconformities at Deep Sea Drilling Project Site 548, Goban Spur, *Initial Rep. Deep Sea Drill. Proj.*, 80, 539-555, 1985.
- Poore, R. Z., Middle Eocene through Quaternary planktonic foraminifers from the southern Angola Basin: Deep Sea Drilling Project Leg 73, *Initial Rep. Deep Sea Drill. Proj.*, 73, 429-448, 1984.
- Poore, R. Z., and R. K. Matthews, Late Eocene-Oligocene oxygen and carbon isotope record from South Atlantic Ocean DSDP Site 522, *Initial Rep. Deep Sea Drill. Proj.*, 73, 725-736, 1984.
- Pujol, C., Cenozoic planktonic foraminiferal biostratigraphy of the southwestern Atlantic (Rio Grande Rise): Deep Sea Drilling Project Leg 72, *Initial Rep. Deep Sea Drill. Proj.*, 72, 623-674, 1983.
- Savin, S. M., R. G. Douglas, and F. G. Stehli, Tertiary marine paleotemperatures, *Geol. Soc. Am. Bull.*, 86, 1499-1510, 1975.
- Shackleton, N. J., and J. P. Kennett, Paleotemperature history of the Cenozoic and initiation of Antarctic glaciation: Oxygen and carbon isotopic analyses in DSDP Sites 277, 279, and 281, *Initial Rep. Deep Sea Drill. Proj.*, 29, 743-755, 1975.
- Shackleton, N. J., and N. D. Opdyke, Oxygen isotopic and palaeomagnetic stratigraphy of equatorial Pacific core V28-238: Oxygen isotope temperatures and ice volume on a 10⁵ to 10⁶ year scale, *Quat. Res.*, 3, 39-55, 1973.
- Tauxe, L., P. Tucker, N. P. Petersen, and J. L. LaBrecque, Magnetostratigraphy of Leg 73 sediments, *Palaeogeogr. Palaeoclimatol. Palaeoecol.*, 42, 65-90, 1983.
- Tauxe, L., P. Tucker, N. P. Peterson, and J. L. LaBrecque, Magnetostratigraphy of Leg 73 sediments, *Initial Rep. Deep Sea Drill. Proj.*, 73, 609-612, 1984.

M. D. Feigenson and R. K. Olsson, Department of Geological Sciences, Rutgers University, New Brunswick, N.J. 08903.

D. V. Kent and K. G. Miller, Lamont-Doherty Geological Observatory of Columbia University, Palisades, N.Y. 10964.

(Received November 16, 1987;
revised March 11, 1988;
accepted March 16, 1988.)